Environmental Pollution 243 (2018) 177–188

Contents lists available at ScienceDirect

Environmental Pollution

journal homepage: www.elsevier.com/locate/envpol

Photocatalytic degradation of DOM in urban stormwater runoff with TiO_2 nanoparticles under UV light irradiation: EEM-PARAFAC analysis and influence of co-existing inorganic ions☆

Chen Zhao [a, b], Zhihua Wang [a, *], Chaoyang Wang [b], Xiang Li [b], Chong-Chen Wang [b, **]

[a] State Key Laboratory of Chemical Resource Engineering, Beijing University of Chemical Technology, Beijing, 100029, China
[b] Beijing Key Laboratory of Functional Materials for Building Structure and Environment Remediation, Beijing University of Civil Engineering and Architecture, Beijing, 100044, China

ARTICLE INFO

Article history:
Received 10 June 2018
Received in revised form
14 August 2018
Accepted 20 August 2018
Available online 27 August 2018

Keywords:
Stormwater runoff
Dissolved organic matter
EEM-PARAFAC
Photocatalytic degradation
Inorganic ions

ABSTRACT

In situ photocatalytic degradation of dissolved organic matter (DOM) of stormwater runoff can efficiently improve the aquatic environment quality and relieve the wastewater treatment pressure. In this work, photocatalytic degradation of DOM in TiO_2 (AEROXIDE® P-25) photocatalyst under illumination of ultraviolet (UV) light was carried out, considering the influence of various factors like TiO_2 dosage, solution pH along with the existence of co-existing ions (Cu^{2+} and $H_2PO_4^-$). Generally, the variations of dissolved organic carbon (DOC), UV-based parameters and peak intensities of fluorescent constituents with UV exposure time fitted perfectly with the pseudo-first-order kinetics model. The total DOM removal efficiency was affected by diversiform factors like adsorption capacity of TiO_2, UV light utilization efficiency, reactive free radicals produced and the influence of co-existing ions. The results of fluorescence excitation-emission matrix (EEM) coupled with parallel factor analysis (PARAFAC) modeling demonstrated that all the photodegradation rates for three identified fluorescent constituents (protein-like constituent 1 and 3, humic-like constituent 2) were faster than UV-absorbing chromophores, suggesting the DOM molecules in urban stormwater runoff contained much more π^*-π transition structures. In addition, $H_2PO_4^-$ ions affected the photodegradation of DOM by capturing positive holes (h^+) and hydroxyl radical ($\cdot OH$), whereas Cu^{2+} ions were inclined to generate Cu-protein complexes that were more difficult to degrade than the other Cu-DOM complexes. This study supplied novel insights into the photocatalytic degradation mechanism of individual organic constituent in urban stormwater runoff and explored the influences of co-existing contaminants on their adsorption-photocatalysis processes.

1. Introduction

With the acceleration of urbanization, the problem of urban stormwater runoff pollution has become a hot topic discussed by researchers and engineers (Goonetilleke et al., 2005; Hong et al., 2017; Mcelmurry et al., 2014). In stormwater system, dissolved organic matter (DOM) is mainly composed of organic substances with multiple functional groups and molecular sizes (Chen et al., 2002; Santos et al., 2012; Zhao et al., 2015; Zhao et al., 2016). DOM compositions and structures are influenced by their sources and biogeochemical processes. (Mcelmurry et al., 2014; Schulten and Gleixner, 1999). As a ubiquitous and reactive fraction, DOM can forcefully interact with the co-existing contaminants and nutrient substances, thus altering their migration, transformation, bioavailability, toxicity and fate (Kieber et al., 2005; Kieber et al., 2004). Furthermore, considering that current methods to protect aquatic environments are massively inoperative and even guided by the “end-of-pipe” operations, the inefficient DOM treatment by former stormwater facilities will significantly increase the difficulty of sewage treatment plants. Previous researches had proved that DOM could lead to the formation of disinfection by products (DBP) and membrane fouling (Zhang et al., 2008).

Among various treatment technologies, heterogeneous photocatalysis employing UV light and TiO_2 catalyst has proved its high-

☆ This paper has been recommended for acceptance by Baoshan Xing.

* Corresponding author.
** Corresponding author.
E-mail addresses: zhwang@mail.buct.edu.cn (Z. Wang), wangchongchen@bucea.edu.cn (C.-C. Wang).

https://doi.org/10.1016/j.envpol.2018.08.062
0269-7491/

efficiency in photodegrading a large number of ambiguous recalcitrant organic substances into unsteadily biodegradable substances. Moreover, under the appropriate conditions, it is possible to ultimately mineralize organic molecules to form pollution-free CO_2 and H_2O (Cai et al., 2018; Li et al., 2018). The dominating reaction mechanism of photocatalysis degradation is based on the generation of clean and environmentally friendly free radicals with strong oxidizing ability (Wang et al., 2017; Zou et al., 2015). As well, the strong stability (including chemical-, thermal- and photostability), the undemanding experimental conditions (ambient temperature and pressure), the efficient recyclability and low operating costs promote wide application of UV/TiO_2 technique in wastewater treatment (Wang et al., 2016; Wang et al., 2014).

In former studies of photocatalytic DOM degradation, dissolved organic carbon (DOC) concentrations and some parameters fitted from UV–visible spectral data were mainly applied as indicators for estimating the total removal efficiency (Rajca and Bodzek, 2013; Zanardi-Lamardo et al., 2004). However, these indexes are insufficient to fully clarify the behaviors of the extremely nonhomogeneous DOM. As a credible and hypersensitized optical instrument, fluorescence spectroscopy can be used to efficiently identify the different types of organic compounds (Baker et al., 2004; Coble, 1996; Her et al., 2003). Furthermore, the photocatalytic DOM decomposition performances have been explored applying fluorescence-based instruments in a range of aquatic environments (Kavurmaci and Bekbolet, 2014; Patel-Sorrentino et al., 2004; Zanardi-Lamardo et al., 2004). However, the previous studies assessed the photodegradation tendency of DOM simply via the analysis of changes in intrinsic fluorescence intensity or peak position, neglecting the possible error caused by the spectral overlaps from a complicated mixture of various fluorescent compounds.

As the most popular stoichiometry technique, parallel factor analysis (PARAFAC) can deconvolute the complicated EEMs spectra into independent fluorescent organic substances that represent different types of fluorophores with similar physicochemical properties and structures (Ishii and Boyer, 2012; Stedmon and Bro, 2008). The EEM-PARAFAC technique has been widely utilized to monitor the activities of various DOM substances in water environments (Hudson et al., 2010; Seredyn'Skasobecka et al., 2011; Stedmon et al., 2011; Yang et al., 2015). The peak locations and intensities of the separate PARAFAC constituent reflect the water quality and treatment performance. Therefore, the photocatalytic degradation behaviors of different constituents can be effectively identified by utilizing EEM-PARAFAC technique, and the overlaps between various fluorescents will be effectively avoided. It is noteworthy that Phong and Hur (2015) explored the photodegradation behaviors of different fluorescents by EEM-PARAFAC, in which the litter-derived DOM, Elliott soil humic acid and Pony lake fulvic acid were selected as DOM references. But up to now, few researchers applied EEM-PARAFAC technique to investigate the adsorption-photocatalytic processes and mechanism of urban stormwater runoff DOM in UV/TiO_2 system.

More importantly, dissolved inorganic ions are quite ubiquitous in DOM-containing urban stormwater runoff (Brown and Peake, 2006; Gammons et al., 2005; Zhao et al., 2017). They may appreciably affect the photocatalytic reactions for DOM disposal. Therefore, it is important to explore the influences of different inorganic species on photocatalytic DOM decomposition in UV/TiO_2 system, which will be beneficial to clarify the photocatalytic degradation mechanism of DOM in real stormwater runoff samples. This study will aim (1) to demonstrate the practicability of the environmentally friendly and cost effective UV/TiO_2 system for the elimination of DOM in urban stormwater runoff, (2) to compare the variations in DOC concentrations, UV parameters and fluorescents identified by EEM-PARAFAC of urban stormwater runoff DOM in UV/TiO_2 system under different experimental conditions, including TiO_2 doses and pH values, and (3) to examine the effects of co-existing inorganic ions (Cu^{2+} and $H_2PO_4^-$) that are common in stormwater runoff on DOM degradation with TiO_2 as catalyst under UV light illumination.

2. Materials and methods

2.1. Sampling and pretreatment

The runoff water samples were collected directly with 1000 mL fully cleaning glass containers after the generation of surface runoff on 2nd August of 2017 at a regular sampling point of Daxing campus (39°51′ N, 116°24′ E) of Beijing University of Civil Engineering and Architecture (BUCEA). The sampling site was covered by asphalt pavement, and the pavement precipitates, uncleaned waste and the other organic substances washed by rainfall could be the potential DOM sources. Weather parameters like quantity of precipitation, rainfall duration, ground temperature, air dampness, dry period, atmospheric pressure and catchment area were shown in Table 1. The stormwater runoff samples were qualified for the corresponding analyses because the rainfall event matched well with the standard of EPA US (Smullen et al., 2003).

All types of glassware were dipped in NaOH solution (0.1 M) for 30 min before sampling, then cleaned by distilled water, subsequently another immersion in HNO_3 solutions (4.0 M) for 1 d, finally treated with ultrapure water. After sampling, the samples were filtered with 0.45 μm PTFE filter and measured immediately. The background concentrations of co-existing contaminants of the filtered DOM samples were shown in Table S1. Subsequent analysis must ensure that the extracted DOM samples were restored to room temperature.

2.2. Reagents and instruments

AEROXIDE® P-25, a type of commercial TiO_2 purchased from InnoChem Corporation (Beijing, China), was selected as photocatalyst, whose specific surface area and the average particle diameter was reported to be $50 \pm 15\ m^2\ g^{-1}$ and 21 nm, respectively (Phong and Hur, 2015). The point zero of charge (PZC) of the AEROXIDE® P-25 was 6.25 (Singh et al., 2008). Other analytical grade reagents were commercially available and used without any further pretreatment. The solutions like 4.0 M HNO_3, 0.1 M HCl, 0.1 M NaOH, 1000.0 mg L^{-1} $NaHCO_3$, 1000.0 mg L^{-1} Na_2CO_3, 1000.0 mg L^{-1} potassium biphthalate, 0.01 M $CuCl_2$ and 0.01 M NaH_2PO_4 solutions were prepared with ultrapure water.

DOC was calculated from the difference between total carbon (TC) and total inorganic carbon (TIC) determined on a Jena multi N/C 3100 analyzer (Zhao et al., 2015; Zhao et al., 2017). All the values were reported as the mean values of three parallel measurements.

The UV–visible absorption spectra of the DOM were measured on a Perkin-Elmer lambda 650S spectrophotometer. DOM samples with ultra-absorptive UV light will be diluted with ultrapure water to make A_{300} (the absorbance at 300 nm) less than 0.02 to eliminate inner filter effect (Green and Blough, 1994; Yang and Hur, 2014). Ultrapure water was selected as the blank control of the UV–visible absorption spectra.

EEM spectra were detected by a Hitachi F-7000 Fluorescence spectrophotometer, with both emission wavelengths and excitation wavelengths ranging from 200 to 550 nm (Muller et al., 2008; Para et al., 2011). Both Rayleigh and Raman scatterings were eliminated by zeroing the measured EEMs data in the two triangle regions at $E_m \leq Ex + 20$ nm and $E_m \geq 2E_x - 10$ nm) (Stedmon and Bro, 2008), and by deducting the ultrapure water blank spectra, respectively (Santos et al., 2009). Relative precisions of UV–visible and EEMs

Table 1
The weather parameters of the sampling day (2nd August of 2017).

Quantity of precipitation (mm)	Rainfall duration (min)	Air dampness (%)	Atmospheric pressure (in mmHg)	Catchment area (m^2)	Ground temperature (°C)	Antecedent dry period (d)
33.7	232	92	28.64	253	21	7

measurements were routinely controlled within 2% (Santos et al., 2012).

2.3. Photocatalytic experiments

The photocatalytic experiments for removal of the DOM substances were conducted at ambient conditions in 50 mL quartz bottles. The bottles were placed in the photochemical reaction system (PCX-50A, Beijing Perfectlight Co. Ltd.) equipped with nine identical LED lamps ($\lambda = 385$ nm, power density = 300 mW cm^{-2}). Under the condition of the fixed DOM concentration (approximately 10 mg L^{-1}), the effects of different TiO_2 doses (10, 20, 30, 40 mg) on photocatalytic experiments were investigated. Before the UV irradiation, 0.1 M HCl or NaOH solutions were applied to regulate the pH of DOM aqueous solutions, stirring in the dark for 60 min to achieve the adsorption-desorption equilibrium between TiO_2 and DOM (Phong and Hur, 2015). In addition, the liquid-solid heterogeneous photocatalytic reaction system was also prepared by addition of inorganic ions (Cu^{2+} and $H_2PO_4^-$) at optimal TiO_2 dose and pH value to examine their effects on the photocatalytic DOM degradation. During the 4 h photocatalytic degradation experiments, 20 mL aliquots were extracted using a 0.45 μm PTFE filter to determine the residual DOM concentration, in which the pH values were regulated to 7.0 prior to subsequent analysis (Valencia et al., 2013).

2.4. PARAFAC modeling

PARAFAC modeling utilizes the chemometrics principles to decompose the EEM spectral dataset into separate fluorescent constituents and to provide the relative contents of different fluorophores (Bro, 1997; Ohno et al., 2008; Stedmon and Bro, 2008). In this application, original EEM fluorescent data were composed of three-ways arrays of X with $I \times J \times K$, where I, J, K are the amount of samples, emission wavelengths, and excitation wavelengths, respectively. The EEM-PARAFAC model can be expressed as Eq (1):

$$X_{ijk} = \sum_{f=1}^{F} a_{if} b_{jf} c_{kf} + \varepsilon_{ijk} \quad i = 1...\mathrm{I}\ \ \mathrm{j} = 1...\mathrm{J}\ k = 1...K \qquad (1)$$

where F defines the numerical order of fluorophores in this model, X_{ijk} is the fluorescent peak intensity of the ith sample at the jth dependent variable (emission wavelength) and kth dependent variable (excitation wavelength). a_{if} is in proportion to the content of the fth fluorophore in the ith sample. b_{jf} is a rateable assessment of the fluorescence quantum efficiency of the fth fluorophore. Similarly, c_{kf} is linearly related to the specific absorption coefficient at excitation wavelength k. Finally, ε_{ijk} is the residual matrix, which is used to minimize the sum of squared residuals by alternating least squares algorithm (Stedmon et al., 2003).

EEM-PARAFAC dataset (495 samples × 55 emissions × 55 excitations) was operated via the N-way toolbox in the MATLAB 7.1 computation program (Kowalczuk et al., 2009; Stedmon and Bro, 2008). The fluorescent intensity of individual organic constituent was described by F_{max}, which can represent the relative contents of individual constituent. The data was divided into two independent parts and calculated independently. The PARAFAC models (2–8 types of constituents) were then obtained from the two datasets independently. Accuracy and reliability of the model were performed by contrasting the spectral shapes of the fluorescent constituents derived by the two separated datasets.

3. Results and discussion

3.1. Variations of DOC concentrations during photocatalytic degradation

DOC is the most comprehensive and frequently-used parameter that can quantify the amount of DOM in water systems, because organic substances in natural environment generally represent a significant fraction of the carbonaceous organic constituents (Croué et al., 2003). The variation trends of DOC concentrations in adsorption and photocatalysis processes under UV light illumination were shown in Fig. 1. Without TiO_2 as photocatalyst, DOC concentrations of urban stormwater runoff exhibited minimal variations at pH being 7 upon UV light illumination after 4 h. However, when TiO_2 was used as the photocatalyst, the total removal characterized by DOC increased to 46–71% according to various TiO_2 loadings and solution pH values. Being compared to the optimal condition, the presence of Cu^{2+} or $H_2PO_4^-$ ions can inhibit the processes of adsorption and photodegradation of DOM, the total removal of DOC reduced to 19–47%. Furthermore, an uncomplicated pseudo-first-order kinetics model has been applied to depict the photocatalytic degradation of DOM in the recent researches (Abargues et al., 2018; Zhang et al., 2017). In this research, most of the changed trends of the DOC concentrations conformed to the pseudo-first-order kinetics model ($R^2 = 0.95$–0.98), while the experiment with the presence of Cu^{2+} did not fit the model well (R^2 was approximately 0.75). The results revealed that the coexisting Cu^{2+} species might exert negative impact to the DOM degradation via competitive effects with oxidizing free radicals or forming hardly degradable substances (Cai et al., 2003). In addition, even after the 4 h irradiation, the DOM in urban stormwater runoff was not fully mineralized in DOC concentrations, suggesting that a large amount of the DOM molecules might be resistant to UV light, or they may convert into the other organic substances that were more difficult to be photodegraded (Cho and Choi, 2002).

3.1.1. Influences of TiO_2 loading for adsorption-photodegradation reactions

Influences of TiO_2 loading (0.00, 0.25, 0.50, 0.75, 1.00 g L^{-1}) for this reaction system were investigated at pH = 7 without coexisting ions (as illustrated in Fig. 1(a) and (b)). As expected, the gradual increase of TiO_2 dosages (ranged from 0.25 to 1.00 g L^{-1}) enhanced their adsorption capacities toward DOC (rose from 4.49% to 12.32%), presumably due to the enhancive total adsorption sites of TiO_2 particles. With the increase of TiO_2 dosage up to 0.75 g L^{-1}, the removal efficiency and the apparent photodegradation rates calculated by DOC concentrations increased correspondingly. With respect to the maximum loading (1.00 g L^{-1}) applied in this work, the total removal efficiency and the rate constant were significantly decreased than that of TiO_2 dosage = 0.75 g L^{-1}. The reason for the decrease of photocatalytic efficiency under higher catalyst loading might be the excessive amount of TiO_2 particles can produce light

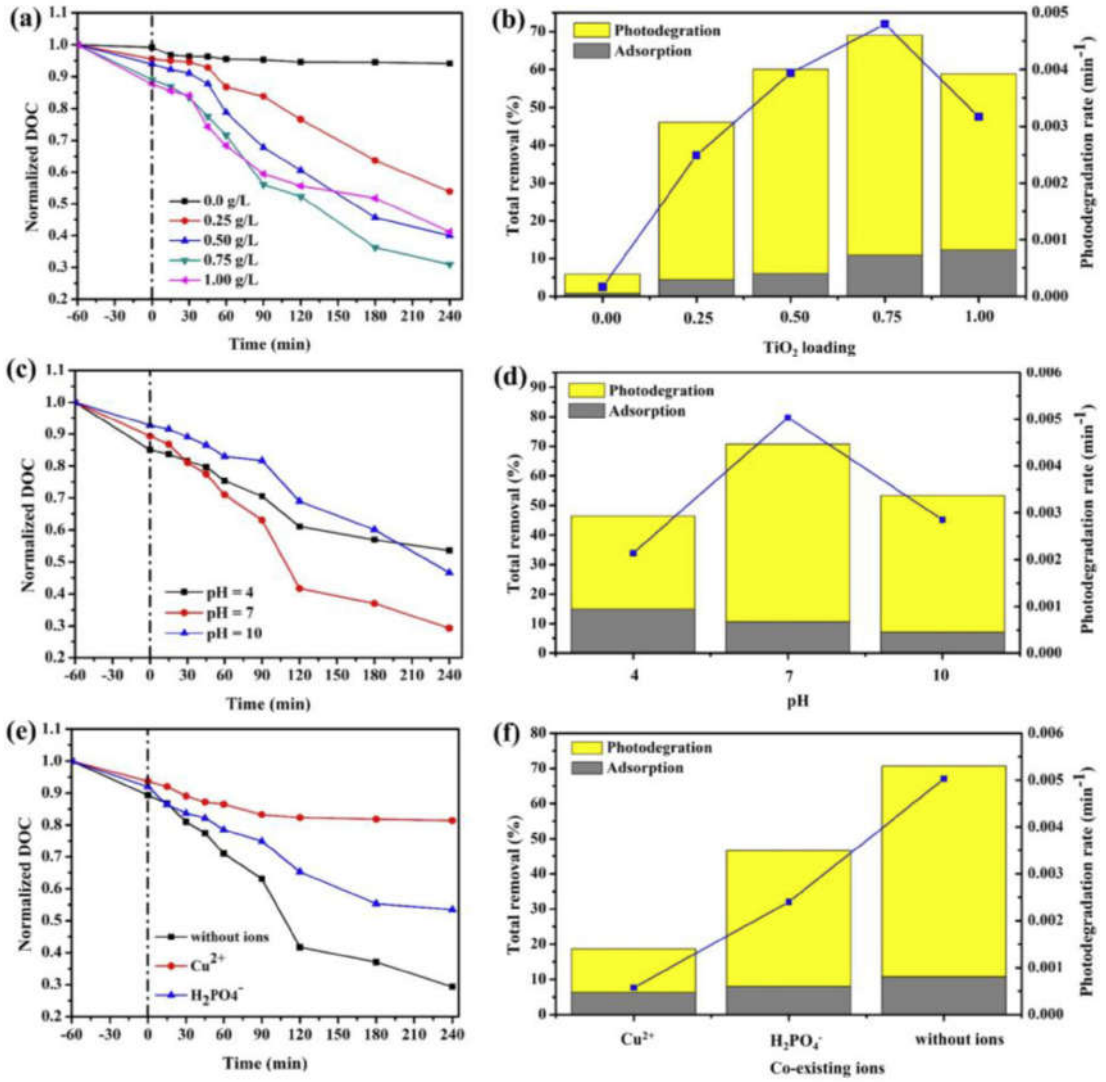

Fig. 1. (a), (c) and (e) adsorption-photocatalytic curves of DOC under different TiO_2 loadings, pH values and the presence/absence of co-existing ions; (b), (d) and (f) degree of adsorption, photodegradation and photocatalytic rates of DOC under different TiO_2 loadings, pH values and the absence/presence of co-existing ions.

screening effect that reduced the adsorption and utilization efficiency of UV light, thus affecting the photocatalytic processes (Gaya and Abdullah, 2008; Meng et al., 2010). The turbidity measured in this research were 898, 1964, 2640 and 3176 NTU for the photocatalyst dosages increasing from 0.25 to 1.00 g L^{-1}. Previous studies have demonstrated that the optimal dosage of TiO_2 particles varied depending on the styles of photocatalytic reactor and the chemical compositions of organic substances (Fu et al., 2006; Phong and Hur, 2015), therefore, any selected dosage should be manipulated below the saturation level of the specific photocatalyst to guarantee effective photons absorption.

3.1.2. *Influences of solution pH values for adsorption-photodegradation reactions*

The influences of pH on the photocatalytic degradation of DOM in urban stormwater runoff were investigated at solution pH being 4, 7 and 10 under the optimal TiO_2 loading (0.75 g L^{-1}). As illustrated in Fig. 1(c) and (d), the adsorptive capacities of TiO_2 reinforced with the increasement of solution pH values (up to pH = 10), which can be interpreted by the charge property of DOM and the PZC of TiO_2. When operating pH = 4 < PZC (6.25), the surface charge of TiO_2 became positively charged and gradually absorbed the DOM with negative charge via electrostatic interactions (Safiur Rahman et al., 2013; Yan et al., 2013). At pH = 10 > PZC (6.25), the TiO_2 surface was negatively charged and exerted the reverse force to DOM in urban stormwater runoff. Surprisingly, the maximum adsorption capacity of TiO_2 (pH = 4) did not achieve the optimal removal efficiency. The overall removal efficiency calculated by DOC concentrations at pH = 4, 7, 10 was 46.39, 70.69 and 53.33%, respectively. Moreover, the photodegradation rates of DOC were 0.00214, 0.00503 and 0.00285 min^{-1}, following the order pH being 7 > pH being 10 > pH being 4. The inconformity between the adsorption capacity of DOC and the total removal efficiency might be due to surface behaviors of TiO_2 particles, the aggregation of TiO_2 particles, and the decrease of free radicals with oxidizing ability in the DOM solutions. The former studies verified that the interaction between DOM molecules and TiO_2 particles could lead to the conversion of the photochemical characteristics of the TiO_2 surface (Phong and Hur, 2015; Yang et al., 2009). The decrease of pH led to the aggregation of TiO_2 particles, which reduces the photons utilization efficiency (Palmer et al., 2002). The interpretation is partly affirmed by the turbidity values measured at different pH

values, namely that the turbidity values were 2237, 2549, 2865 NTU at pH = 4, 7 and 10, respectively. Meanwhile, because of the complicated structures and large molecular weight of DOM molecules, photogenerated holes (h^+) with powerful oxidation ability can directly degrade the DOM constituents adsorbed on the surface of TiO_2 into smaller organic fragments. Therefore, the oxidation of the smaller molecules produced during the photocatalytic processes and other non-UV-adsorbing organic substances was the rate limiting step of this reaction system. More advantageous production of ·OH through the hole oxidation of OH^- in the solution at neutral and alkaline conditions (Franch et al., 2002; Nguyen et al., 2003), contributed to more efficient ·OH attack toward DOM in urban stormwater runoff and subsequently higher photocatalytic degradation rates.

3.1.3. Influences of co-existing ions for adsorption-photodegradation reactions

The concentrations of Zn^{2+}, Cu^{2+}, N-containing and P-containing ions in urban stormwater runoff were much higher than the other co-existing inorganic ions (as shown in Table S1). However, previous studies had demonstrated that Zn^{2+} and NO_3^- had negligible influences on photocatalytic oxidation of organic substances over UV illuminated TiO_2 (Abdullah et al., 1990; Butler and Davis, 1993; Chen and Liu, 2007). Therefore, Cu^{2+} and $H_2PO_4^-$ ions were selected as the model cation and anion to explore their influences on adsorption-photocatalytic degradation of urban stormwater runoff DOM under UV/TiO_2 systems (Erickson et al., 2012; Lee and Bang, 2000; Walker et al., 1999). In this study, the 0.01 M $CuCl_2$ and NaH_2PO_4 solutions were prepared to explore the influences of co-existing ions (Cu^{2+} and $H_2PO_4^-$) on the photodegradation of DOM. As shown in Fig. 1(e) and (f), the adsorption of DOC slightly decreased with existence of Cu^{2+} and $H_2PO_4^-$ at pH = 7. The overall DOC removal and degradation rates decreased on the order of Cu^{2+} > $H_2PO_4^-$ > without ions. The results may be attributed to the presence of Cu^{2+} suppressed the mineralization of DOM in urban stormwater runoff, significantly in relation to the resistance of DOM-Cu complexes to oxidation (Uyguner and Bekbolet, 2010). Okonomoto and co-workers proved that Cu^{2+} can only strengthen the photocatalytic performance at its concentration up to 0.0001 M, while further increases in its concentration weaken the overall reaction efficiency (Okamoto et al., 1985). However, the free and adsorbed $H_2PO_4^-$ reacted with positive h^+ and ·OH to generate H_2PO_4· (as shown in Eqs (2) and (3)), which was less active than ·OH and h^+ (Hu et al., 2003). Therefore, the excess $H_2PO_4^-$ had an inhibition influence for the photocatalytic degradation of DOM in urban stormwater runoff.

$$H_2PO_4^- + \bullet OH \rightarrow H_2PO_4^{\bullet} + OH^- \quad (2)$$

$$H_2PO_4^- + h^+ \rightarrow H_2PO_4^{\bullet -} \quad (3)$$

3.2. Changes in UV parameters during adsorption-photodegradation reactions

Before investigating the changes of UV-related parameters during the whole reactions, the differences in spectroscopic properties between stormwater runoff and typical water DOM were compared. The parameters for comparison were spectral slope coefficients (S), the specific ultraviolet absorbance at 254 or 280 nm ($SUVA_{254}$ or $SUVA_{280}$), the fluorescence index (FI), the humification index (HIX) and the biological index (BIX) (the calculation details of the corresponding parameters were shown in Electronic Supplementary Information). They can provide information about molecular weight (Singh et al., 2008), aromaticity (Weishaar et al., 2003), source (Mcknight et al., 2001), humification degree (Huguet et al., 2009) and biological activity (Huguet et al., 2010), respectively. As shown in Table 2, the S values of DOM in urban stormwater runoff were minimum (9.32–9.57 μm^{-1}), suggesting that the average molecular weight of DOM in urban stormwater runoff was relatively larger. Oppositely, the $SUVA_{280}$ values in this study were in the range of 3.10–3.16 L mg C^{-1} m^{-1} ($SUVA_{254}$ was applied in the rest of studies), which were much higher than those in the other water environments, indicating that DOM in urban stormwater runoff contained much more aromatic structures. Furthermore, the fluorescence properties of DOM in different water environments were similar except that the higher humification degree was found in some lake, fogwater and sediment pore water DOM samples. It was well known that HIX values greater than 10 typically indicated strong humification (Huguet et al., 2009). Therefore, the fluorescence results revealed that the DOM in stormwater runoff had weak humic character with both terrigenous and microbial contribution.

The concentrations of a large number of contaminants in aquatic environment, such as lignin, tannic acid, fulvic/humic acid and large amounts of aromatic organic substances can be characterized by UV_{254} values (Altmann et al., 2016; Kulovaara et al., 1996). Thus, UV_{254} can be regarded as a reasonable parameter for detecting the photodegradation efficiency of DOM (Meng et al., 2013; Saadi et al., 2006). Without the influence of co-existing ions, the photodegradation rates calculated by UV_{254} values basically fitted the pseudo-first-order kinetics model (R^2 = 0.81–0.98), and the total removal efficiency was relatively higher than those of DOC based experiments, ranging from 76.24 to 93.40%. Moreover, there was a positive correlation between UV_{254} values and the DOC concentrations (R^2 = 0.76–0.85), suggesting that chromophoric DOM substances were the important and ubiquitous contributors to the DOC pool in stormwater runoff. It is noteworthy that the trends of the DOM adsorption degree with different TiO_2 doses, pH values and the presence of co-existing ions were same for the UV_{254} and DOC values (as shown in Fig. 2(a)-(f)). However, the adsorptive removal calculated by UV_{254} values (21.83–42.15%) were much higher than characterized by DOC concentrations (7.26–14.97%) under the identical experimental conditions, which may be due to the terminal functional groups (such as hydroxyl and carboxyl) of aromatic compounds reinforced the adoption affinity of the surfaces of TiO_2 particles (Tachikawa et al., 2003; Tachikawa et al., 2004). Comparing with DOC based experiments, the total removal with the presence of Cu^{2+} ions increased dramatically when using UV_{254} values to monitor photocatalytic reaction process (Fig. 2 (f)). As the UV_{254} mainly represents the content of aromatic substances in aquatic environment, the results suggested that the Cu^{2+} ions in urban stormwater runoff may react with the other non-UV-absorbing and macromolecular substances that were difficult to photocatalytic degradation. Yuan and co-workers (Yuan et al., 2017) applied 2D-COS technique to demonstrate that protein-like substances in stormwater runoff preferentially chelated with Cu^{2+} ions, indicating that Cu-protein complexes may be the major resistant substances in this experimental system.

In addition, the photodegradation rates on the basis of UV_{254} (0.0025–0.0078 min^{-1}, the median was 0.0057 min^{-1}) were congruously higher than the DOC based experiments (0.0005–0.0048 min^{-1}, the median was 0.0029 min^{-1}), revealing that the chromophores in DOM mainly contained macromolecular sized aromatic constituents, could be quickly decomposed into micro-molecular sized non-aromatic compounds (Sanly et al., 2007). To further confirm this hypothesis, S and the $SUVA_{280}$ were estimated through the entire adsorption-photocatalysis process under the optimal condition (TiO_2 dose = 0.75 g L^{-1}, pH = 7). The variation trends of S and $SUVA_{280}$ values with reaction time were

Table 2
Summary of spectroscopic characteristics of DOM in typical water environment systems.

Samples	*S*	*SUVA*	FI	HIX	BIX	References
	μm^{-1}	L mg C^{-1} m^{-1}				
Stormwater runoff	9.32–9.57	3.10–3.16	1.58–1.67	4.38–4.92	0.78–0.85	This study
Sea water	15.10–38.80	0.596–1.22	1.48–1.77	0.92–4.60	0.74–1.38	(Helms et al., 2013)
River water	13.10–14.00	0.36–2.68	1.68–1.95	0.75–0.79	0.75–0.83	(Xu et al., 2016)
Lake water	13.80–22.90	0.70–2.90	1.60–1.80	2.00–8.10	–	(Phong et al., 2014)
Fogwater	–	0.15–0.79	1.42–1.83	1.76–6.79	0.64–1.02	(Birdwell and Valsaraj, 2010)
Drinking water	–	1.50–3.00	1.41–1.63	0.85–0.93	0.54–0.79	(Lavonen et al., 2015)
Sediment pore water	–	0.20–1.50	1.10–1.80	0.7–7.6	0.7–1.0	(Chen et al., 2015)

illustrated in Fig. 2 (g) and (h). The initial value of *S* was 9.57 μm^{-1}, which was similar to the previous results of the *S* values in urban stormwater runoff reported by Zhao et al. (2015, 2016). Moreover, the *S* values dramatically increased with reaction time and the terminal value reached to 58.71 μm^{-1}, implying that organic compounds with high molecular weight were gradually degraded and finally formed relatively smaller molecular compounds. In contrast, the $SUVA_{280}$ values showed the opposite trend to *S*, the initial value of $SUVA_{280}$ was 3.16 L mg C^{-1} m^{-1} and the terminal value was only 0.17 L mg C^{-1} m^{-1}. The above results demonstrated that aromatic moieties in DOM of urban stormwater runoff were preferentially removed and a large proportion of chromophoric substances might be transformed into non-UV-absorbing structures via adsorption-photocatalysis processes.

3.3. PARAFAC constituents and their behaviors during adsorption-photocatalysis reactions

3.3.1. EEM fluorescent constituents identified by PARAFAC technique

Three independent fluorophores (C1, C2 and C3) were resolved by the PARAFAC modeling based on the original 495 EEM spectra from 55 independent experiments (Fig. 3(a)-(c)). Moreover, the excitation and emission loadings accurately confirmed the peak locations of the three constituents (as shown in Fig. 3(d)-(f)). Constituent 1 (C1) exhibited a fluorescent peak at Ex/Em wavelength pair of 230/350 nm. Similar constituents were previously assigned to a protein-like or a tryptophan-like (peak T) constituent, such as aromatic amino acids (Chen et al., 2003; Coble, 1996; Korshin et al., 2018; Stedmon and Markager, 2005; Wu et al., 2011). This constituent mainly originated from anthropogenic input and correlated to terrestrial fluorescent materials (Carstea et al., 2010; Yamashita et al., 2008). Constituent 2 (C2) can be described as two peaks (peak A and C) with excitation wavelength at 250 nm and 300 nm, along with an emission wavelength at 440 nm, indicating the existence of a humic-like fluorescence (Coble, 1996; Huang et al., 2015) or a FA (fulvic acid)-like constituent with aromatic terrestrial structures and macromolecular weight (Santín et al., 2009). In consideration of disadvantages caused by the traditional peak picking method (peak shifting and overlapping), infallible distinctions between two types of humic substances at peaks A and C cannot be made, thus leading to UV humic-like compounds turned out to be the dominating fluorescent constituents in the DOM of urban stormwater runoff samples in the former studies (Zhao et al., 2015; Zhao et al., 2016; Zhao et al., 2017). This significant result confirmed the diversity of organic compositions in urban stormwater runoff and provided valuable references for subsequent studies. Constituent 3 (C3), another protein-like constituent, was characterized by peaks at 275/313 nm. It was defined as tyrosine-like fluorophore and attributed to traditional peak B (Yamashita and Jaffé, 2011; Yamashita and Tanoue, 2003). However, a red shift occurred in the maximum peak position as being compared to the peak B described by Coble (1996), suggesting that the aromaticity of tyrosine-like substances in urban stormwater runoff was stronger than those present in freshwater/marine environments (Banaitis et al., 2006), and it might integrate with the structural condensation and ploymerization of DOM.

3.3.2. Photocatalytic degradation of individual fluorescent constituent at different conditions

Just like DOC and UV_{254} experiments, the whole of decomposed fluorescent constituents showed stronger adsorption capacity under higher TiO_2 doses, lower pH values and without the influence of co-existing ions conditions (as illustrated in Fig. 4(a)-(i)). It is noteworthy that the remarkable decreases with UV irradiation were uniformly detected for all the PARAFAC fluorophores, suggesting that every identified fluorophore was affected by the direct photochemical degradation reaction (Phong and Hur, 2015). The photodegradation rates of the identified constituents match well with the pseudo-first-order kinetics calculated by the F_{max} values with R^2 being 0.82–0.99. Considering that the degradation behaviors of the three identified constituents followed the first order exponential decay process, which was proven to be a successful expression for DOM photocatalysis degradation with irradiation time (Del Vecchio and Blough, 2002), thus the photocatalytic degradation changes of the C1, C2 and C3 constituents with their kinetic rates can be compared directly. Without the influences of co-existing ions on photocatalytic oxidation process, the total removal efficiencies of the three identified fluorophores ranged from 83.06 to 99.40% (as listed in Table 3).

When there was no TiO_2 in the reaction system, the total removal ratios in the F_{max} values of the C1, C2 and C3 also reached to 10.23, 21.54 and 13.52%, and the rates corresponded to 0.00043, 0.00096 and 0.00059 min^{-1}, respectively (as shown in Table 3), following the order of C2 > C3 > C1, which contrasted with the negligible self-photodegradation process characterized by DOC values. This phenomenon revealed that fluorophores were more sensitive to the UV illumination than the rest of non-fluorescent organic substances, indicating that fluorophores can be used as a powerful proof to monitor the subtle changes of organic substances in stormwater runoff. Furthermore, the above results were in line with the previous researches on photo-bleaching DOM samples collected from the other water environments (Hur et al., 2011; Moran and Sheldon, 2000; Mostofa et al., 2007), in which the protein-like fluorophores were more refractory to photocatalytic degradation than the A, M, C fluorophores. The more interesting findings in this study were that the total removal efficiencies characterized by the individual fluorophore peak of DOM in urban stormwater runoff were uniformly stronger than those of DOC, along with that the photodegradation rates were higher than DOC and UV_{254} based experiments (Table 3). Comparing with the UV-absorbing chromophores, the faster photocatalytic degradation of fluorophores may be due to the fluorescence was caused by the π^*-π transitions in organic molecules and its fast disappearance upon UV light illumination (Phong and Hur, 2015).

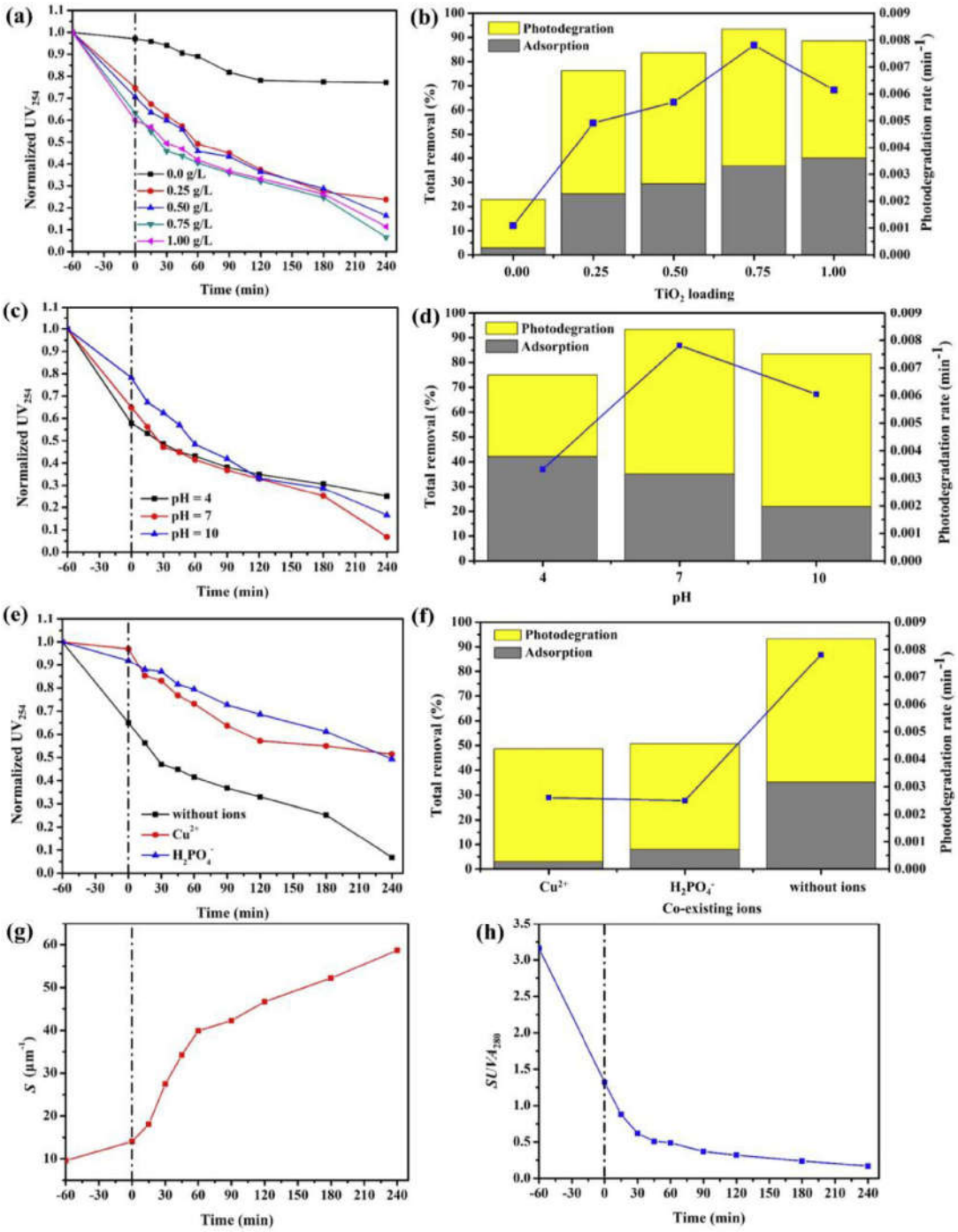

Fig. 2. (a), (c) and (e) adsorption-photocatalytic curves of UV_{254} under different TiO_2 loadings, pH values and the presence/absence of co-existing ions; (b), (d) and (f) degree of adsorption, photodegradation and photocatalytic rates of UV_{254} under different TiO_2 loadings, pH values and the absence/presence of co-existing ions; (g)–(h) development of *S* and $SUVA_{280}$ values during adsorption and photodegradation reactions.

When TiO_2 was present in the reaction system, the total removal ratios of the C1, C2 and C3 constituent reached 95.37, 99.40, and 96.34% under the optimum condition (TiO_2 dose = 0.75 g L^{-1}, pH = 7, without co-existing ions), the degradation rates complied with the order of C2 > C3 > C1 (Table 3). The photocatalytic degradation behaviors of the identified fluorophores can be elucidated by counterparts (Chen et al., 2014; Schneider et al., 2014). The suppositional mechanism of this photocatalytic degradation process was shown in Fig. 5, briefly, e^- and h^+ pairs are produced in conduction and valence band upon illumination, and photocatalytic processes for the degradation of DOM are initiated by the formation of reactive free radicals by photo-generated h^+ and e^- on surface of TiO_2. In this study, h^+ may oxide water molecules or hydroxyl ions to generate ·OH, which oxidized most of the DOM molecules existed in the solution. The adsorption degree of C2 constituent onto TiO_2 nanoparticles was lower than the others, resulting in a large proportion of C2 constituent can be photodegraded by ·OH present in the solution and the maximum photodegradation rate

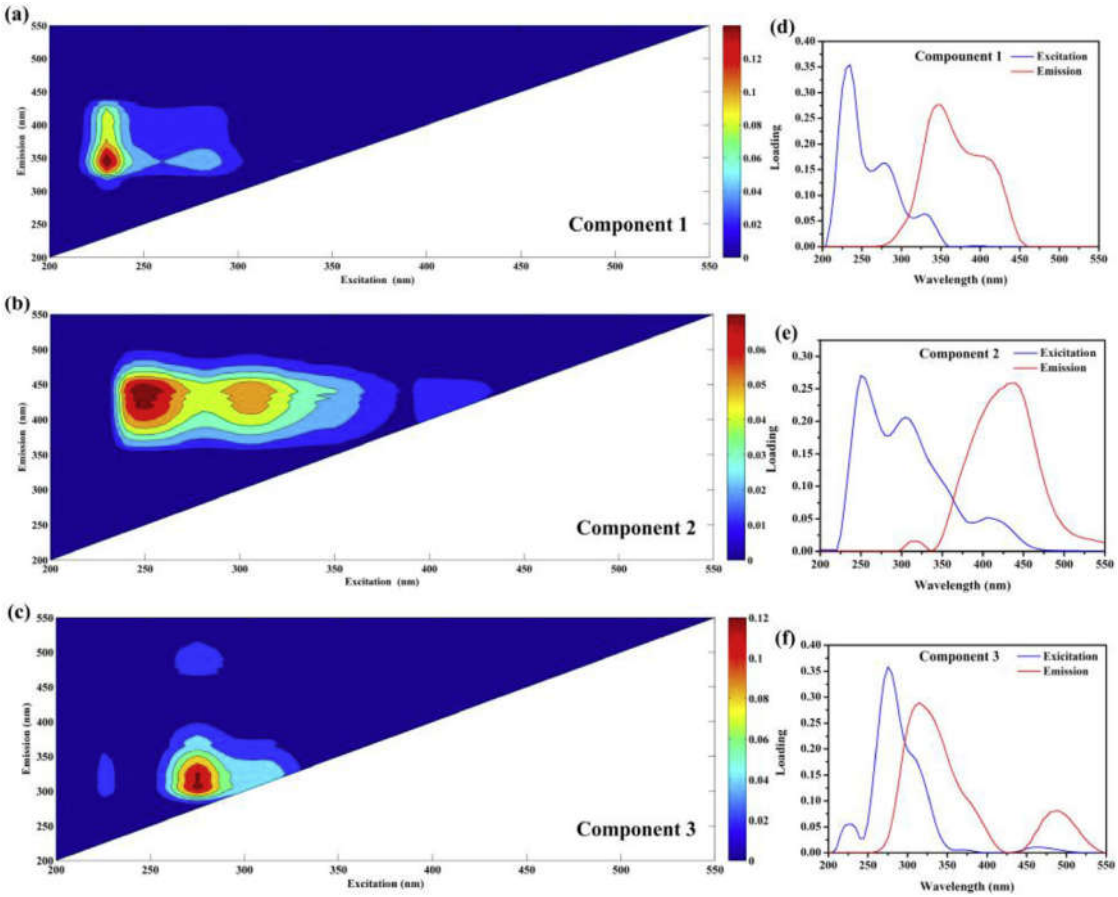

Fig. 3. EEM fluorescence constituents, excitation (blue lines) and emission loadings (red lines) identified by the DOM Fluor-PARAFAC model.

among the three fluorophores. In the other words, the higher adsorption degree of C1 and C3 constituents onto TiO_2 nanoparticles can also lead to the reduction in active sites and photons utilization in reactio system, thus inhibiting the photodegradation of C1 and C3 constituents (Fu et al., 2018; Liu et al., 2016; Zhao et al., 2018).

Meanwhile, the reactive h^+ may directly participate in oxidation processes and decompose macromolecular organic substances into smaller fragments. Furthermore, the photo-induced e^- reacted with dissolved oxygen to generate $\cdot O_2^-$, which can also oxidize the DOM molecules. In addition, the UV light absorption by individual fluorescent constituents facilitated to the generation of reactive intermediates like singlet oxygen ($^1O_2$) and the triplet states of DOM (^{3}DOM*). ^{3}DOM* may react with target organic substances directly through electron and energy transfer, thus imposing the great influence on UV degradation of the identified fluorophores (Lester et al., 2013).

The adsorption and photocatalytic degradation processes of the three constituents were dramatically suppressed with the presence of Cu^{2+} and $H_2PO_4^-$ ions, suggesting that the fluorescent organic substances had the similar physicochemical properties as other non-absorbing compounds. Moreover, the inhibitory effects of $H_2PO_4^-$ on the three fluorescent constituents were identical, evidenced by that the total removal ratios of C1, C2 and C3 increased to 64.33, 72.84 and 71.04%, respectively (Table 3). These results can be contributed to h^+ and ·OH radicals were captured by $H_2PO_4^-$, the oxidation capacity of $H_2PO_4\cdot$ free radicals was much weaker than the other radicals (Hu et al., 2003). However, as shown in Fig. 4(g)-(i), the inhibitory effects of Cu^{2+} ions on the protein-like constituents (C1 and C3) were stronger than the humic-like or fulvic-like constituent (C2). Croué and co-workers (Croué et al., 2003) applied XAD-4 and XAD-8 resins to demonstrated that Cu^{2+} ions primarily reacted with the low-affinity functional groups of humic constituents, whereas the functional groups containing nitrogen element similar to those of peptides and amino acids were inclined to chelate with Cu^{2+} ions to generate relatively stable complexes in natural aquatic systems. Therefore, the results proved that Cu-protein complexes were more difficult to photodegrade, further affirming the assumption in UV_{254} values.

4. Conclusions

The fundamental behaviors of DOM in urban stormwater runoff with the changes of TiO_2 dosages during adsorption-photodegradation processes were identical for DOC, UV_{254} and EEM: the faster reduction corresponding to higher TiO_2 loadings. But the decreases of photodegrading ratios at excess TiO_2 loading were attributed to the reduced absorption efficiency of the TiO_2 particles resulting from the enhancive turbidity. The prominent changes of DOM photocatalytic rates with different solution pH values were attributed to surface modification of the photocatalyst by different adsorptive degrees, the aggregation of TiO_2 particles, and the production of oxidizing free radicals. The changes in DOC, UV_{254} and individual constituent identified by PARAFAC matched well with the pseudo-first-order kinetics. The photodegradation rates calculated by DOC concentrations were lower than UV_{254} and fluorescence peak-based experiments, revealing the preferential removal of aromatic substances under UV illumination. This study

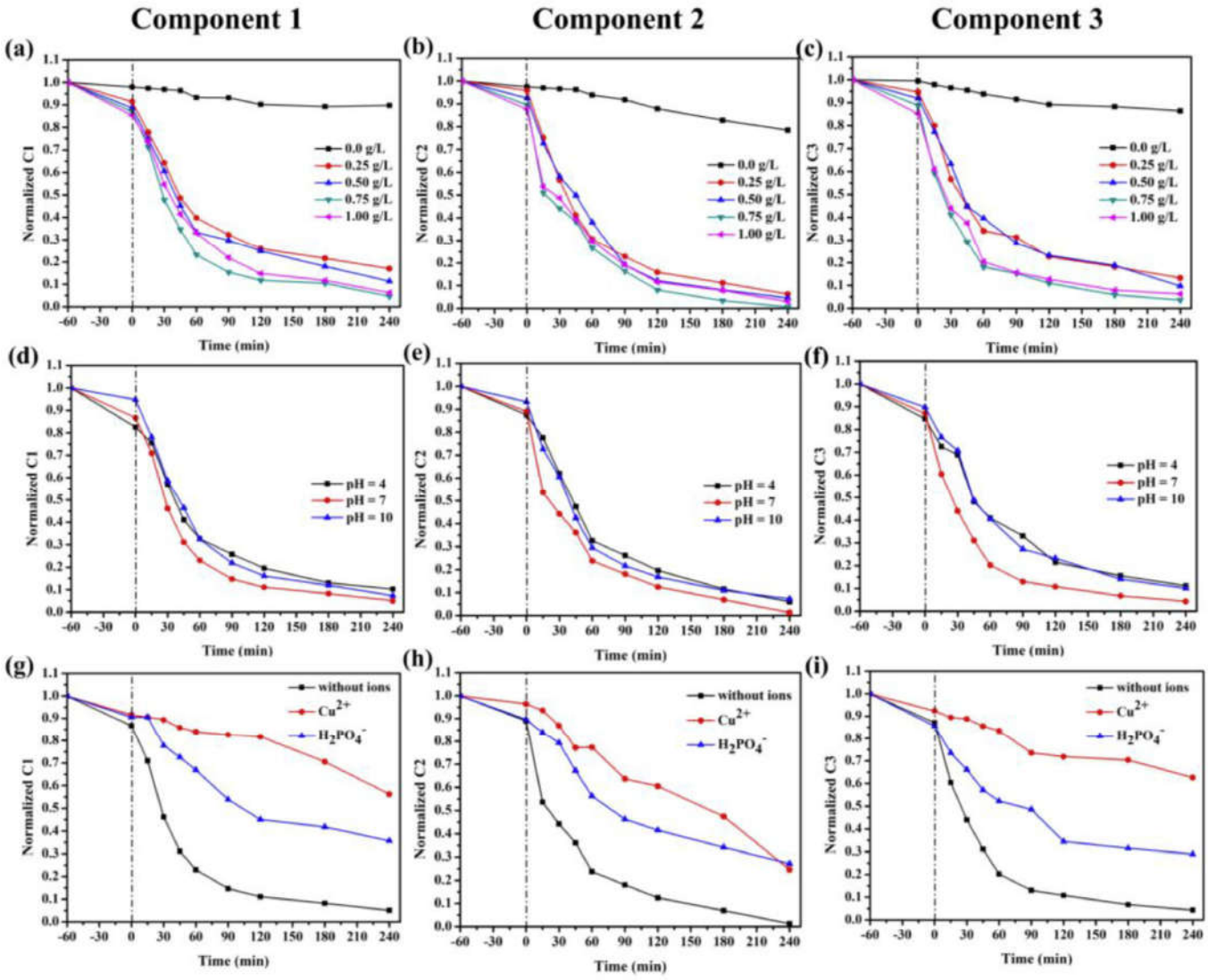

Fig. 4. Changes in normalized parameters during 1-hour of adsorption and 4-hours of photocatalytic degradation of C1, C2, C3 fluorescent constituents in urban stormwater runoff with different TiO_2 loadings, pH values and co-existing ions.

Table 3
Experimental data related to adsorption-photocatalysis processes of the three identified PARAFAC constituents.

No.	Experimental conditions			Adsorption (%)			Photocatalytic degradation (%)			Total removal efficiency (%)			Photodegradation rates (min^{-1})		
	TiO_2 ($g\ L^{-1}$)	pH	co-existing ions	C1	C2	C3	C1	C2	C3	C1	C2	C3	C1	C2	C3
1	0.0	7.0	–	1.98	2.52	0.50	8.25	19.02	13.03	10.23	21.54	13.53	0.00043	0.00096	0.00059
2	0.25	7.0	–	8.59	4.13	5.33	74.47	89.56	81.38	83.06	93.69	86.71	0.00695	0.01102	0.00787
3	0.50	7.0	–	11.36	7.48	8.44	77.27	87.95	82.07	88.63	95.43	90.51	0.00817	0.01293	0.00882
4	0.75	7.0	–	13.09	10.46	11.16	82.28	88.94	85.18	95.37	99.40	96.34	0.01178	0.01955	0.01270
5	1.00	7.0	–	14.68	12.30	14.86	79.04	84.70	78.80	93.72	97.00	93.66	0.01078	0.01324	0.01073
6	0.75	4.0	–	17.43	12.42	15.33	72.32	81.60	73.49	89.75	94.02	88.82	0.00896	0.01111	0.00874
7	0.75	7.0	–	13.31	10.98	12.91	81.62	87.70	82.76	94.93	98.68	95.67	0.01164	0.01877	0.01215
8	0.75	10.0	–	5.24	6.74	10.23	87.41	85.97	79.66	92.65	92.71	89.89	0.00874	0.01215	0.00940
9	0.75	7.0	–	13.22	10.68	12.32	80.24	86.70	81.96	93.46	92.64	94.28	0.01124	0.01815	0.01185
10	0.75	7.0	Cu^{2+}	8.42	3.57	7.66	35.37	71.85	29.72	43.79	75.15	37.38	0.00186	0.00522	0.00162
11	0.75	7.0	$H_2PO_4^-$	9.50	10.34	14.43	54.82	62.50	59.61	64.32	72.84	76.93	0.00415	0.00513	0.00457

affirmed the practical applications of EEM-PARAFAC method to explore the different responses and the behaviors originated from different fluorescent constituents in urban stormwater runoff upon photocatalytic degradation. Comparing with protein-like constituents (C1 and C3), the humic or fulvic-like constituent (C2) was more effectively removed during adsorption-photodegradation processes mainly due to its direct oxidative degradation by ·OH. More importantly, the presence of Cu^{2+} and

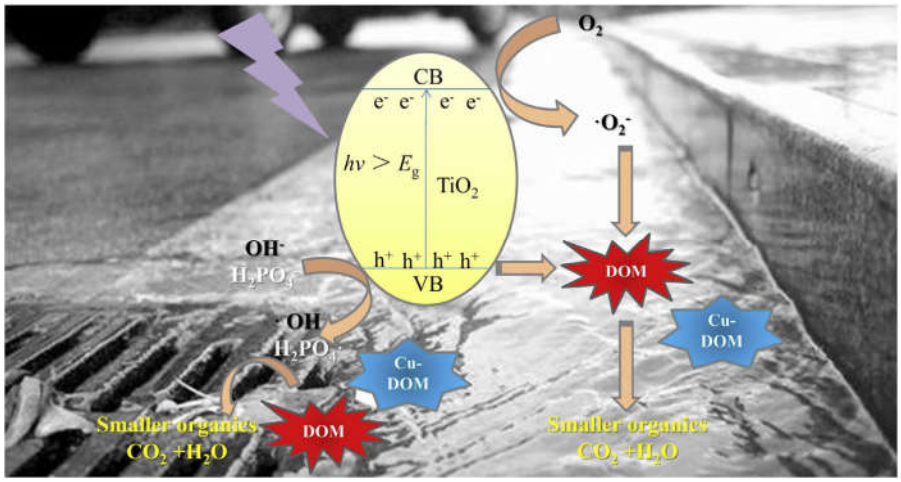

Fig. 5. Possible reaction mechanism for the photocatalytic oxidation of DOM in urban stormwater runoff over TiO_2 particles.

$H_2PO_4^-$ were detrimental for the photodegradation DOM in urban runoff. The $H_2PO_4^-$ ions inhibited the photocatalytic performance of the TiO_2 by capturing h^+ and ·OH. But Cu^{2+} ions were inclined to generate refractory Cu-DOM complexes with protein-like constituents to reduce photocatalytic efficiency. In general, this study showed that EEM-PARAFAC method can be used as a valuable tool for investigating the photocatalytic mechanisms of various organic constituents in urban stormwater runoff. Considering the low photon and quantum utilization efficiencies of TiO_2 particles, further researches should to develop new photocatalysts that can be utilized in photodegradation of DOM in aquatic environments under visible or UV–visible irradiation.

Acknowledgments

We thank the financial support from Project of Construction of Innovation Teams and Teacher Career Development for Universities and Colleges Under Beijing Municipality (IDHT20170508), Great Wall Scholars Training Program Project of Beijing Municipality Universities (CIT&TCD20180323), Beijing Talent Project (2017A38), the Fundamental Research Funds for Beijing Universities of Civil Engineering and Architecture (X18075/X18076/X18124/X18125/X18276) and Scientific Research Foundation of Beijing University of Civil Engineering and Architecture (KYJJ2017033/KYJJ2017008).

Appendix A. Supplementary data

Supplementary data related to this article can be found at https://doi.org/10.1016/j.envpol.2018.08.062

References

Abargues, M.R., Giménez, J.B., Ferrer, J., Bouzas, A., Seco, A., 2018. Endocrine disrupter compounds removal in wastewater using microalgae: degradation kinetics assessment. Chem. Eng. J. 334, 313–321.
Abdullah, M., Low, G.K.C., Matthews, R.W., 1990. Effects of common inorganic anions on rates of photocatalytic oxidation of organic carbon over illuminated titanium dioxide. J. Phys. Chem. 94 (17), 6820–6825.
Altmann, J., Massa, L., Sperlich, A., Gnirss, R., Jekel, M., 2016. UV254 absorbance as real-time monitoring and control parameter for micropollutant removal in advanced wastewater treatment with powdered activated carbon. Water Res. 94, 240–245.
Baker, A., Ward, D., Lieten, S.H., Periera, R., Simpson, E.C., Slater, M., 2004. Measurement of protein-like fluorescence in river and waste water using a hand-held spectrophotometer. Water Res. 38 (12), 2934–2938.
Banaitis, M.R., Waldrip-Dail, H., Diehl, M.S., Holmes, B.C., Hunt, J.F., Lynch, R.P., Ohno, T., 2006. Investigating sorption-driven dissolved organic matter fractionation by multidimensional fluorescence spectroscopy and PARAFAC. J. Colloid Interface Sci. 304 (1), 271–276.
Birdwell, J.E., Valsaraj, K.T., 2010. Characterization of dissolved organic matter in fogwater by excitation-emission matrix fluorescence spectroscopy. Atmos. Environ. 44 (27), 3246–3253.
Bro, R., 1997. PARAFAC. Tutorial and applications. Chemometr. Intell. Lab. 38 (2), 149–171.
Brown, J.N., Peake, B.M., 2006. Sources of heavy metals and polycyclic aromatic hydrocarbons in urban stormwater runoff. Sci. Total Environ. 359 (1), 145–155.
Butler, E.C., Davis, A.P., 1993. Photocatalytic oxidation in aqueous titanium dioxide suspensions: the influence of dissolved transition metals. J. Photochem. Photobiol., A 70 (3), 273–283.
Cai, R., Kubota, Y., Fujishima, A., 2003. Effect of copper ions on the formation of hydrogen peroxide from photocatalytic titanium dioxide particles. J. Catal. 219 (1), 214–218.
Cai, Z., Dwivedi, A.D., Lee, W.-N., Zhao, X., Liu, W., Sillanpaa, M., Zhao, D., Huang, C.H., Fu, J., 2018. Application of nanotechnologies for removing pharmaceutically active compounds from water: development and future trends. Environ. Sci-Nano. 5 (1), 27–47.
Carstea, E.M., Baker, A., Bieroza, M., Reynolds, D., 2010. Continuous fluorescence excitation-emission matrix monitoring of river organic matter. Water Res. 44 (18), 5356–5366.
Chen, S., Liu, Y., 2007. Study on the photocatalytic degradation of glyphosate by TiO_2 photocatalyst. Chemosphere 67 (5), 1010–1017.
Chen, J., Gu, B., Leboeuf, E.J., Pan, H., Dai, S., 2002. Spectroscopic characterization of the structural and functional properties of natural organic matter fractions. Chemosphere 48 (1), 59–68.
Chen, W., Westerhoff, P., Leenheer, J.A., Booksh, K., 2003. Fluorescence excitation-emission matrix regional integration to quantify spectra for dissolved organic matter. Environ. Sci. Technol. 37 (24), 5701–5710.
Chen, D., Zhu, H., Wang, X., 2014. A facile method to synthesize the photocatalytic TiO_2/montmorillonite nanocomposites with enhanced photoactivity. Appl. Surf. Sci. 319 (1), 158–166.
Chen, M., Lee, J.H., Hur, J., 2015. Effects of sampling methods on the quantity and quality of dissolved organic matter in sediment pore waters as revealed by absorption and fluorescence spectroscopy. Environ. Sci. Pollut. Res. 22 (19), 14841–14852.
Cho, Y., Choi, W., 2002. Visible light-induced reactions of humic acids on TiO_2. J. Photochem. Photobiol., A 148 (1–3), 129–135.
Coble, P.G., 1996. Characterization of marine and terrestrial DOM in seawater using excitation-emission matrix spectroscopy. Mar. Chem. 51 (4), 325–346.
Croué, J.P., Benedetti, M.F., Violleau, D., Leenheer, J.A., 2003. Characterization and copper binding of humic and nonhumic organic matter isolated from the South Platte River: evidence for the presence of nitrogenous binding site. Environ. Sci. Technol. 37 (2), 328–336.
Del Vecchio, R., Blough, N.V., 2002. Photobleaching of chromophoric dissolved organic matter in natural waters: kinetics and modeling. Mar. Chem. 78 (4), 231–253.
Erickson, A.J., Gulliver, J.S., Weiss, P.T., 2012. Capturing phosphates with iron enhanced sand filtration. Water Res. 46 (9), 3032–3042.
Franch, M.I., Ayllón, J.A., Peral, J., Domènech, X., 2002. Photocatalytic degradation of short-chain organic diacids. Catal. Today 76 (2–4), 221–233.
Fu, J., Ji, M., Wang, Z., Jin, L., An, D., 2006. A new submerged membrane photocatalysis reactor (SMPR) for fulvic acid removal using a nano-structured photocatalyst. J. Hazard Mater. 131 (1–3), 238–242.
Fu, J., Kyzas, G.Z., Cai, Z., Deliyanni, E.A., Liu, W., Zhao, D., 2018. Photocatalytic degradation of phenanthrene by graphite oxide-TiO_2-Sr$(OH)_2$/$SrCO_3$ nanocomposite under solar irradiation: effects of water quality parameters and

predictive modeling. Chem. Eng. J. 335, 290–300.
Gammons, C.H., Shope, C.L., Duaime, T.E., 2005. A 24 h investigation of the hydrogeochemistry of baseflow and stormwater in an urban area impacted by mining: butte, Montana. Hydrol. Process. 19 (14), 2737–2753.
Gaya, U.I., Abdullah, A.H., 2008. Heterogeneous photocatalytic degradation of organic contaminants over titanium dioxide: a review of fundamentals, progress and problems. J. Photoch. Photobio. C 9 (1), 1–12.
Goonetilleke, A., Thomas, E., Ginn, S., Gilbert, D., 2005. Understanding the role of land use in urban stormwater quality management. J. Environ. Manag. 74 (1), 31–42.
Green, S.A., Blough, N.V., 1994. Optical absorption and fluorescence properties of chromophoric dissolved organic matter in natural waters. Limnol. Oceanogr. 39 (8), 1903–1916.
Helms, J.R., Stubbins, A., Perdue, E.M., Green, N.W., Chen, H., Mopper, K., 2013. Photochemical bleaching of oceanic dissolved organic matter and its effect on absorption spectral slope and fluorescence. Mar. Chem. 155, 81–91.
Her, N., Amy, G., McKnight, D., Sohn, J., Yoon, Y., 2003. Characterization of DOM as a function of MW by fluorescence EEM and HPLC-SEC using UVA, DOC, and fluorescence detection. Water Res. 37 (17), 4295–4303.
Hong, N., Zhu, P., Liu, A., 2017. Modelling heavy metals build-up on urban road surfaces for effective stormwater reuse strategy implementation. Environ. Pollut. 231, 821–828.
Hu, C., Yu, J.C., Hao, Z., Wong, P.K., 2003. Effects of acidity and inorganic ions on the photocatalytic degradation of different azo dyes. Appl. Catal. B Environ. 46 (1), 35–47.
Huang, S.B., Wang, Y.X., Ma, T., Tong, L., Wang, Y.Y., Liu, C.R., Zhao, L., 2015. Linking groundwater dissolved organic matter to sedimentary organic matter from a fluvio-lacustrine aquifer at Jianghan Plain, China by EEM-PARAFAC and hydrochemical analyses. Sci. Total Environ. 529, 131–139.
Hudson, N., Baker, A., Reynolds, D., 2010. Fluorescence analysis of dissolved organic matter in natural, waste and polluted waters—a review. River Res. Appl. 23 (6), 631–649.
Huguet, A., Vacher, L., Relexans, S., Saubusse, S., Froidefond, J.M., Parlanti, E., 2009. Properties of fluorescent dissolved organic matter in the Gironde Estuary. Org. Geochem. 40 (6), 706–719.
Huguet, A., Vacher, L., Saubusse, S., Etcheber, H., Abril, G., Relexans, S., Ibalot, F., Parlanti, E., 2010. New insights into the size distribution of fluorescent dissolved organic matter in estuarine waters. Org. Geochem. 41 (6), 595–610.
Hur, J., Jung, K.Y., Jung, Y.M., 2011. Characterization of spectral responses of humic substances upon UV irradiation using two-dimensional correlation spectroscopy. Water Res. 45 (9), 2965–2974.
Ishii, S.K.L., Boyer, T.H., 2012. Behavior of reoccurring PARAFAC components in fluorescent dissolved organic matter in natural and engineered systems: a critical review. Environ. Sci. Technol. 46 (4), 2006–2017.
Kavurmaci, S.S., Bekbolet, M., 2014. Tracing TiO_2 photocatalytic degradation of humic acid in the presence of clay particles by excitation-emission matrix (EEM) fluorescence spectra. J. Photochem. Photobiol., A 282 (15), 53–61.
Kieber, R.J., Skrabal, S.A., Smith, C., Willey, J.D., 2004. Redox speciation of copper in rainwater: temporal variability and atmospheric deposition. Environ. Sci. Technol. 38 (13), 3587–3594.
Kieber, R.J., Skrabal, S.A., Smith, B.J., Willey, J.D., 2005. Organic complexation of Fe(II) and its impact on the redox cycling of iron in rain. Environ. Sci. Technol. 39 (6), 1576–1583.
Korshin, G.V., Sgroi, M., Ratnaweera, H., 2018. Spectroscopic surrogates for real time monitoring of water quality in wastewater treatment and water reuse. Curr. Opin. Env. Sust. 2, 12–19.
Kowalczuk, P., Durako, M.J., Young, H., Kahn, A.E., Cooper, W.J., Gonsior, M., 2009. Characterization of dissolved organic matter fluorescence in the South Atlantic Bight with use of PARAFAC model: interannual variability. Mar. Chem. 113 (3–4), 182–196.
Kulovaara, M., Corin, N., Backlund, P., Tervo, J., 1996. Impact of UV_{254} -radiation on aquatic humic substances. Chemosphere 33 (5), 783–790.
Lavonen, E.E., Kothawala, D.N., Tranvik, L.J., Gonsior, M., Schmitt-Kopplin, P., Köhler, S.J., 2015. Tracking changes in the optical properties and molecular composition of dissolved organic matter during drinking water production. Water Res. 85, 286–294.
Lee, J.H., Bang, K.W., 2000. Characterization of urban stormwater runoff. Water Res. 34 (6), 1773–1780.
Lester, Y., Sharpless, C.M., Mamane, H., Linden, K.G., 2013. Production of photooxidants by dissolved organic matter during UV water treatment. Environ. Sci. Technol. 47 (20), 11726–11733.
Li, F., Du, P., Liu, W., Li, X., Ji, H., Duan, J., Zhao, D., 2018. Hydrothermal synthesis of graphene grafted titania/titanate nanosheets for photocatalytic degradation of 4-chlorophenol: solar-light-driven photocatalytic activity and computational chemistry analysis. Chem. Eng. J. 331, 685–694.
Liu, W., Cai, Z., Zhao, X., Wang, T., Li, F., Zhao, D., 2016. High-capacity and photoregenerable composite material for efficient adsorption and degradation of phenanthrene in water. Environ. Sci. Technol. 50 (20), 11174–11183.
Mcelmurry, S.P., Long, D.T., Voice, T.C., 2014. Stormwater dissolved organic matter: influence of land cover and environmental factors. Environ. Sci. Technol. 48 (1), 45–53.
Mcknight, D.M., Boyer, E.W., Westerhoff, P.K., Doran, P.T., Kulbe, T., Andersen, D.T., 2001. Spectrofluorometric characterization of dissolved organic matter for indication of precursor organic material and aromaticity. Limnol. Oceanogr. 46 (1), 38–48.
Meng, N.C., Bo, J., Chow, C.W.K., Saint, C., 2010. Recent developments in photocatalytic water treatment technology: a review. Water Res. 44 (10), 2997–3027.
Meng, F., Huang, G., Yang, X., Li, Z., Li, J., Cao, J., Wang, Z., Sun, L., 2013. Identifying the sources and fate of anthropogenically impacted dissolved organic matter (DOM) in urbanized rivers. Water Res. 47 (14), 5027–5039.
Moran, M.A., Sheldon Jr., W.M., 2000. Carbon loss and optical property changes during long-term photochemical and biological degradation of estuarine dissolved organic matter. Limnol. Oceanogr. 45 (6), 1254–1264.
Mostofa, K.M.G., Yoshioka, T., Konohira, E., Tanoue, E., 2007. Photodegradation of fluorescent dissolved organic matter in river waters. Geochem. J. 41 (5), 323–331.
Muller, C.L., Baker, A., Hutchinson, R., Fairchild, I.J., Kidd, C., 2008. Analysis of rainwater dissolved organic carbon compounds using fluorescence spectrophotometry. Atmos. Environ. 42 (34), 8036–8045.
Nguyen, V.N.H., Amal, R., Beydoun, D., 2003. Effect of formate and methanol on photoreduction/removal of toxic cadmium ions using TiO_2 semiconductor as photocatalyst. Chem. Eng. Sci. 58 (19), 4429–4439.
Ohno, T., Amirbahman, A., Bro, R., 2008. Parallel factor analysis of excitation-emission matrix fluorescence spectra of water soluble soil organic matter as basis for the determination of conditional metal binding parameters. Environ. Sci. Technol. 42 (1), 186–192.
Okamoto, K.I., Yamamoto, Y., Tanaka, H., Tanaka, M., Itaya, A., 1985. Heterogeneous photocatalytic decomposition of phenol over TiO_2 powder. Bull. Chem. Soc. Jpn. 58 (7), 2015–2022.
Palmer, F.L., Eggins, B.R., Coleman, H.M., 2002. The effect of operational parameters on the photocatalytic degradation of humic acid. J. Photochem. Photobiol., A 148 (1–3), 137–143.
Para, J., Coble, P.G., Charrière, B., Tedetti, M., Fontana, C., Sempéré, R., 2011. Fluorescence and absorption properties of chromophoric dissolved organic matter (CDOM) in coastal surface waters of the northwestern Mediterranean Sea, influence of the Rhône River. Biogeosciences 7 (12), 4083–4103.
Patel-Sorrentino, N., Mounier, S., Lucas, Y., Benaim, J.Y., 2004. Effects of UV-visible irradiation on natural organic matter from the Amazon basin. Sci. Total Environ. 321 (1–3), 231–239.
Phong, D.D., Hur, J., 2015. Insight into photocatalytic degradation of dissolved organic matter in UVA/TiO_2 systems revealed by fluorescence EEM-PARAFAC. Water Res. 87, 119–126.
Phong, D.D., Lee, Y., Shin, K.H., Hur, J., 2014. Spatial variability in chromophoric dissolved organic matter for an artificial coastal lake (Shiwha) and the upstream catchments at two different seasons. Environ. Sci. Pollut. Res. 21 (12), 7678–7688.
Rajca, M., Bodzek, M., 2013. Kinetics of fulvic and humic acids photodegradation in water solutions. Separ. Purif. Technol. 120 (1), 35–42.
Saadi, I., Borisover, M., Armon, R., Laor, Y., 2006. Monitoring of effluent DOM biodegradation using fluorescence, UV and DOC measurements. Chemosphere 63 (3), 530–539.
Safiur Rahman, M., Whalen, M., Gagnon, G.A., 2013. Adsorption of dissolved organic matter (DOM) onto the synthetic iron pipe corrosion scales (goethite and magnetite): effect of pH. Chem. Eng. J. 234, 149–157.
Sanly, Lim, M., Chiang, K., Amal, R., Fabris, R., Chow, C., Drikas, M., 2007. A Study on the removal of humic acid using advanced oxidation processes. Separ. Sci. Technol. 42 (7), 1391–1404.
Santín, C., Yamashita, Y., Otero, X.L., MÁ, Á., Jaffé, R., 2009. Characterizing humic substances from estuarine soils and sediments by excitation-emission matrix spectroscopy and parallel factor analysis. Biogeochemistry 96 (1–3), 131–147.
Santos, P.S.M., Otero, M., Duarte, R.M.B.O., Duarte, A.C., 2009. Spectroscopic characterization of dissolved organic matter isolated from rainwater. Chemosphere 74 (8), 1053–1061.
Santos, P.S., Santos, E.B., Duarte, A.C., 2012. First spectroscopic study on the structural features of dissolved organic matter isolated from rainwater in different seasons. Sci. Total Environ. 426 (2), 172–179.
Schneider, J., Matsuoka, M., Takeuchi, M., Zhang, J., Horiuchi, Y., Anpo, M., Bahnemann, D.W., 2014. Understanding TiO_2 photocatalysis: mechanisms and materials. Chem. Rev. 114 (19), 9919–9986.
Schulten, H.R., Gleixner, G., 1999. Analytical pyrolysis of humic substances and dissolved organic matter in aquatic systems: structure and origin. Water Res. 33 (11), 2489–2498.
SeredynSkasobecka, B., Stedmon, C.A., Boehansen, R., Waul, C.K., Arvin, E., 2011. Monitoring organic loading to swimming pools by fluorescence excitation-emission matrix with parallel factor analysis (PARAFAC). Water Res. 45 (6), 2306–2314.
Singh, H.K., Saquib, M., Haque, M.M., Muneer, M., 2008. Heterogeneous photocatalysed decolorization of two selected dye derivatives neutral red and toluidine blue in aqueous suspensions. Chem. Eng. J. 136 (2), 77–81.
Smullen, J.T., Cave, K.A., Field, R., Sullivan, D., 2003. National Stormwater Runoff Pollution Database.
Stedmon, C.A., Bro, R., 2008. Characterizing dissolved organic matter fluorescence with parallel factor analysis: a tutorial. Limnol Oceanogr. Meth. 6 (11), 572–579.
Stedmon, C.A., Markager, S., 2005. Resolving the variability in dissolved organic matter fluorescence in a temperate estuary and its catchment using PARAFAC analysis. Limnol. Oceanogr. 50 (2), 686–697.
Stedmon, C.A., Markager, S., Bro, R., 2003. Tracing dissolved organic matter in aquatic environments using a new approach to fluorescence spectroscopy. Mar. Chem. 82 (3–4), 239–254.
Stedmon, C.A., Seredyńska-Sobecka, B., Boe-Hansen, R., Le, T.N., Waul, C.K., Arvin, E.,

2011. A potential approach for monitoring drinking water quality from groundwater systems using organic matter fluorescence as an early warning for contamination events. Water Res. 45 (18), 6030–6038.
Tachikawa, T., Tojo, S., Fujitsuka, M., Majima, T., 2003. One-electron oxidation of aromatic sulfides adsorbed on the surface of TiO_2 particles studied by time-resolved diffuse reflectance spectroscopy. Chem. Phys. Lett. 382 (5), 618–625.
Tachikawa, T., Yoshida, A., Tojo, S., Sugimoto, A., Fujitsuka, M., Majima, T., 2004. Evaluation of the efficiency of the photocatalytic one-electron oxidation reaction of aromatic compounds adsorbed on a TiO_2 surface. Chemistry 10 (21), 5345–5353.
Uyguner, C.S., Bekbolet, M., 2010. TiO_2-assisted photocatalytic degradation of humic acids: effect of copper ions. Water Sci. Technol. 61 (10), 2581–2590.
Valencia, S., Marín, J.M., Restrepo, G., Frimmel, F.H., 2013. Application of excitation-emission fluorescence matrices and UV/Vis absorption to monitoring the photocatalytic degradation of commercial humic acid. Sci. Total Environ. 442, 207–214.
Walker, W.J., Mcnutt, R.P., Maslanka, C.A.K., 1999. The potential contribution of urban runoff to surface sediments of the Passaic River: sources and chemical characteristics. Chemosphere 38 (2), 363–377.
Wang, C.C., Li, J.R., Lv, X.L., Zhang, Y.Q., Guo, G., 2014. Photocatalytic organic pollutants degradation in metal-organic frameworks. Energy Environ. Sci. 7 (9), 2831–2867.
Wang, C.C., Du, X.D., Li, J., Guo, X.X., Wang, P., Zhang, J., 2016. Photocatalytic Cr(VI) reduction in metal-organic frameworks: a mini-review. Appl. Catal. B Environ. 193, 198–216.
Wang, Y., Bai, W., Han, S., Wang, H., Wu, Q., Chen, J., Jiang, G., Zhao, Z., Xu, C., Huan, Q., 2017. Promoted photoelectrocatalytic hydrogen production performance of TiO_2 nanowire arrays by Al_2O_3 surface passivation layer. Curr. Catal. 6 (1), 50–56.
Weishaar, J.L., Aiken, G.R., Bergamaschi, B.A., Fram, M.S., Fujii, R., Mopper, K., 2003. Evaluation of specific ultraviolet absorbance as an indicator of the chemical composition and reactivity of dissolved organic carbon. Environ. Sci. Technol. 37 (20), 4702–4708.
Wu, J., Zhang, H., He, P.J., Shao, L.M., 2011. Insight into the heavy metal binding potential of dissolved organic matter in MSW leachate using EEM quenching combined with PARAFAC analysis. Water Res. 45 (4), 1711–1719.
Xu, B., Li, J., Huang, Q., Gong, Q., Li, L., 2016. Impacts of land use patterns and typhoon-induced heavy rainfall event on dissolved organic matter properties in the South Tiaoxi River, China. Environ. Earth Sci. 75 (8), 632–647.
Yamashita, Y., Jaffé, R., 2011. Effects of watershed history on dissolved organic matter characteristics in headwater streams. Ecosystems 14 (7), 1110–1122.
Yamashita, Y., Tanoue, E., 2003. Chemical characterization of protein-like fluorophores in DOM in relation to aromatic amino acids. Mar. Chem. 82 (3), 255–271.
Yamashita, Y., Jaffé, R., Maie, N., Tanoue, E., 2008. Assessing the dynamics of dissolved organic matter (DOM) in coastal environments by excitation emission matrix fluorescence and parallel factor analysis (EEM-PARAFAC). Limnol. Oceanogr. 53 (5), 1900–1908.
Yan, L., Fitzgerald, M., Khov, C., Schafermeyer, A., Kupferle, M.J., Sorial, G.A., 2013. Elucidating the role of phenolic compounds in the effectiveness of DOM adsorption on novel tailored activated carbon. J. Hazard Mater. 262, 100–105.
Yang, L., Hur, J., 2014. Critical evaluation of spectroscopic indices for organic matter source tracing via end member mixing analysis based on two contrasting sources. Water Res. 59 (4), 80–89.
Yang, K., Lin, D., Xing, B., 2009. Interactions of humic acid with nanosized inorganic oxides. Langmuir 25 (6), 3571–3576.
Yang, L., Jin, H., Zhuang, W., 2015. Occurrence and behaviors of fluorescence EEM-PARAFAC components in drinking water and wastewater treatment systems and their applications: a review. Environ. Sci. Pollut. Res. 22 (9), 6500–6510.
Yuan, D.H., Guo, X.J., Xiong, Y., Cui, J., Yin, X.A., Li, Y.Z., 2017. Pollutant-removal performance and variability of DOM quantity and composition with traditional ecological concrete (TEC) and improved multi-aggregate eco-concrete (IMAEC) revetment treatments. Ecol. Eng. 105, 141–149.
Zanardi-Lamardo, E., Moore, C.A., Zika, R.G., 2004. Seasonal variation in molecular mass and optical properties of chromophoric dissolved organic material in coastal waters of southwest Florida. Mar. Chem. 89 (1–4), 37–54.
Zhang, H., Qu, J., Liu, H., Zhao, X., 2008. Isolation of dissolved organic matter in effluents from sewage treatment plant and evaluation of the influences on its DBPs formation. Separ. Purif. Technol. 64 (1), 31–37.
Zhang, Y., Zhang, J., Xiao, Y., Chang, V.W.C., Lim, T.T., 2017. Direct and indirect photodegradation pathways of cytostatic drugs under UV germicidal irradiation: process kinetics and influences of water matrix species and oxidant dosing. J. Hazard Mater. 324, 481–488.
Zhao, C., Wang, C.C., Li, J.Q., Wang, C.Y., Wang, P., Pei, Z.J., 2015. Dissolved organic matter in urban stormwater runoff at three typical regions in Beijing: chemical composition, structural characterization and source identification. RSC Adv. 5 (90), 73490–73500.
Zhao, C., Wang, C.C., Li, J.Q., Wang, C.Y., Zhu, Y.R., Wang, P., Zhang, N., 2016. Chemical characteristics of chromophoric dissolved organic matter in stormwater runoff of a typical residential area, Beijing. Desalin. Water Treat. 57, 19727–19740.
Zhao, C., Wang, C.C., Li, J.Q., Wang, P., Ou, J.Q., Cui, J.R., 2017. Interactions between copper(II) and DOM in the urban stormwater runoff: modeling and characterizations. Environ. Technol. 39 (1), 120–129.
Zhao, X., Du, P., Cai, Z., Wang, T., Fu, J., Liu, W., 2018. Photocatalysis of bisphenol A by an easy-settling titania/titanate composite: effects of water chemistry factors, degradation pathway and theoretical calculation. Environ. Pollut. 232, 580–590.
Zou, J.P., Ma, J., Luo, J.M., Yu, J., He, J., Meng, Y., Luo, Z., Bao, S.K., Liu, H.L., Luo, S.L., Luo, X.B., Chen, T.C., Suib, S.L., 2015. Fabrication of novel heterostructured few layered WS_2-Bi_2WO_6/$Bi_{3.84}W_{0.16}O_{6.24}$ composites with enhanced photocatalytic performance. Appl. Catal. B Environ. 179, 220–228.